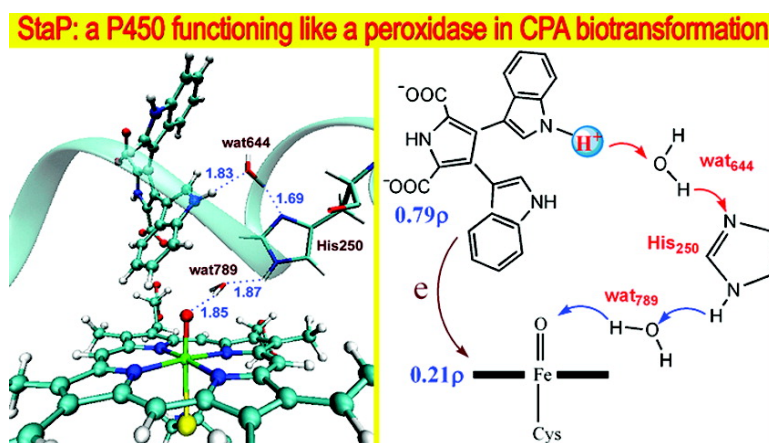


Electron Transfer Activation of Chromopyrrolic Acid by Cytochrome P450 En Route to the Formation of an Antitumor Indolocarbazole Derivative: Theory Supports Experiment

Yong Wang, Hajime Hirao, Hui Chen, Hiroyasu Onaka, Shingo Nagano, and Sason Shaik
J. Am. Chem. Soc., **2008**, 130 (23), 7170-7171 • DOI: 10.1021/ja711426y • Publication Date (Web): 16 May 2008

Downloaded from <http://pubs.acs.org> on February 8, 2009



More About This Article

Additional resources and features associated with this article are available within the HTML version:

- Supporting Information
- Links to the 2 articles that cite this article, as of the time of this article download
- Access to high resolution figures
- Links to articles and content related to this article
- Copyright permission to reproduce figures and/or text from this article

[View the Full Text HTML](#)

Electron Transfer Activation of Chromopyrrolic Acid by Cytochrome P450 En Route to the Formation of an Antitumor Indolocarbazole Derivative: Theory Supports Experiment

Yong Wang,[†] Hajime Hirao,[†] Hui Chen,[†] Hiroyasu Onaka,^{§,¶} Shingo Nagano,[‡] and Sason Shaik^{*,†}

The Institute of Chemistry and The Lise Meitner-Minerva Center for Computational Quantum Chemistry, The Hebrew University of Jerusalem, 91904 Jerusalem, Israel, Biometal Science Laboratory, RIKEN, SPring-8 Center, Harima Institute, Hyogo 679-5148, Japan, Department of Biotechnology, Faculty of Engineering, and Biotechnology Research Center, Toyama Prefectural University, Toyama 939-0398, Japan

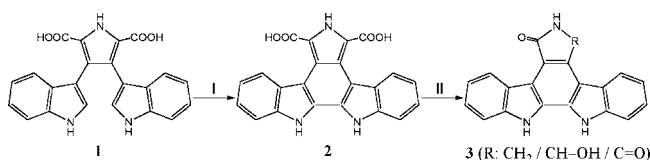
Received December 27, 2007; E-mail: sason@yfaat.ch.huji.ac.il

P450 StaP (CYP245A1) belongs to the family of cytochromes P450^{1a} and catalyzes the formation of staurosporine from chromopyrrolic acid (CPA, **1** in Scheme 1).^{1b} There is a recent surge of interest in this enzyme because of the anticancer activity of staurosporine and also because of the unusual transformation that involves aryl–aryl coupling and oxidative decarboxylation, rather than the usual oxygen insertion performed by most P450s. The origin of this transformation is the focus of the paper.

Mechanistic studies have shown that the carboxylic acid groups in CPA are necessary since the reaction does not take place in their absence.² Subsequent studies³ indicated that the enzyme catalyzes first the C–C bond formation to yield **2**, presumably by double hydrogen abstraction, followed by nonenzymatic reactions leading to the final product **3**. However, since the kinetic isotope effects were close to unity, the authors³ concluded that the C–C coupling is not rate controlling. Recently, two of us (S.N. and H.O.) solved the structure of a StaP–CPA complex⁴ and concluded that CPA is held by an array of hydrogen-bonding (H-bonding) interactions, which keep CPA distant from the heme and would not allow the putative active species, Compound I (Cpd I), to approach CPA sufficiently close to abstract a hydrogen atom. Another observation⁴ was the similarity of electrostatic potential around the indole group (proximal to the heme) to the electrostatic potential of cytochrome *c* peroxidase (CcP), where the active species of the enzyme is not a usual Cpd I species but involves the one-electron-reduced species Cpd II and a radical on an adjacent Trp-191 residue.⁵ By this analogy, Makino et al.⁴ hypothesized that the StaP(Cpd I)–CPA complex forms initially a Cpd II species and a radical cation on the proximal indole moiety of CPA, and subsequently, the N–H bonds of the indoles are deprotonated followed by C–C bond formation. This intriguing postulate and the mechanistic uncertainty of the important transformation of a natural product prompted us to carry out hybrid DFT(B3LYP)/MM calculations (details in Supporting Information) of the Cpd I–CPA complex.

Exploratory B3LYP calculations on a model Cpd I/CPA system showed that when the carboxylic acid groups were deprotonated, the dual-ionized CPA (CPA²⁻) transferred an electron to Cpd I. The ionized state of this group in the enzyme was in line with the short O–N/O (Figure S2 in Supporting Information) distances in the X-ray structure and is inferred also from the presence of a salt bridge between the proximal carboxylic group and Arg₆₇, which showed that these acids, much like aspartic acid residues, are ionized

Scheme 1. The CPA (**1**) Transformation to **3**



in the protein. Our B3LYP/MM calculations were performed in the usual manner,⁶ by adding a solvent shell of 16 Å and all the missing hydrogen atoms to the X-ray structure, followed by short MD and MM minimization. This structure underwent QM/MM geometry optimization using a double- ζ basis set, B1, and single-point calculations by a larger triple- ζ basis set augmented by polarization functions, B2. Tests with B3, a basis set with diffuse functions on all electronegative atoms, confirmed the B2 results. All the technical details are given in Supporting Information (SI).

The use of a monoionized CPA (CPA¹⁻) resulted in a normal Cpd I species, whereas the use of CPA²⁻ caused dramatic changes. Figure 1 shows the B3LYP(B1)/MM optimized key structural features of the CPA²⁻ substrate and the iron-oxo porphyrin species within the pocket. A major structural feature in Figure 1a is the extensive network of short H-bonds that claw the carboxylates of CPA to various noted residues and water molecules. Additionally, in Figure 1b, near the iron-oxo, one can see in parentheses a water molecule (wat₇₈₉) H-bonded to the oxo group and to the N–H of His₂₅₀. This water molecule was added to model the water moiety that splits during the formation of the iron-oxo species Cpd I.⁷

As found in the model QM study, here too, there is a substantial charge transfer from CPA to Cpd I. As shown in Figure 2, in the absence/presence of wat₇₈₉, the density of unpaired electrons on CPA is close to 0.58e/0.79e; the rest of the spin density is shifted to the iron-oxo complex. Indeed, the species has three unpaired electrons, two of which occupy the usual $\pi^*(\text{FeO})$ orbitals,⁸ while the third one is in an orbital made from a combination of the porphyrin a_{2u} and the indole π orbital. Improving the basis set to B2 has a minor effect (e.g., the CPA spin density with wat₇₈₉ included is 0.77e; page S19 in SI).

We further examined the role of the H-bonds in shaping the unusual electronic structure in the following ways: (i) changing the protonation site of His₂₅₀ away from the iron-oxo moiety increased the spin density on the porphyrin + thiolate moiety to 0.74e, almost as in the normal Cpd I (see Figure S15 in SI), and (ii) deleting the partial charges of the H-atoms (in residues Ser₁₈₆, Thr₁₈₇, Arg₆₇, and Thr₃₀₅ and in the crystal water molecules wat₇₇₂ and wat₇₈₀) that are H-bonded to the distal carboxylate of CPA (see Figure S13 in SI) moved most of the spin density to CPA.

[†] The Hebrew University of Jerusalem.

[‡] Harima Institute.

[§] Department of Biotechnology, Faculty of Engineering, Toyama Prefectural University.

[¶] Biotechnology Research Center, Toyama Prefectural University.

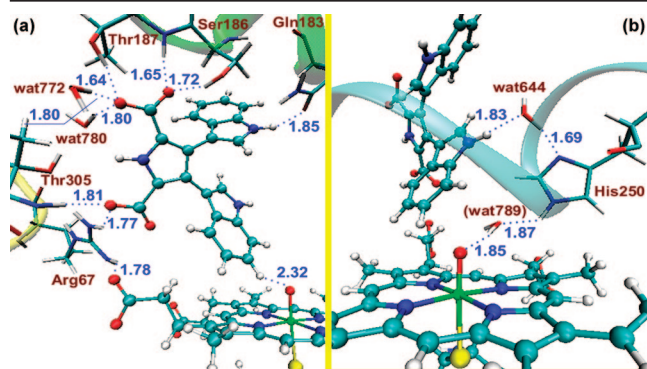


Figure 1. Key B3LYP(B1)/MM optimized distances (Å) of CPA²⁻ and the iron-oxo porphyrin species within StaP. (a) The H-bonding network donated to the carboxyl groups of CPA²⁻. (b) The wat₆₄₄–His₂₅₀–wat₇₈₉ triad.

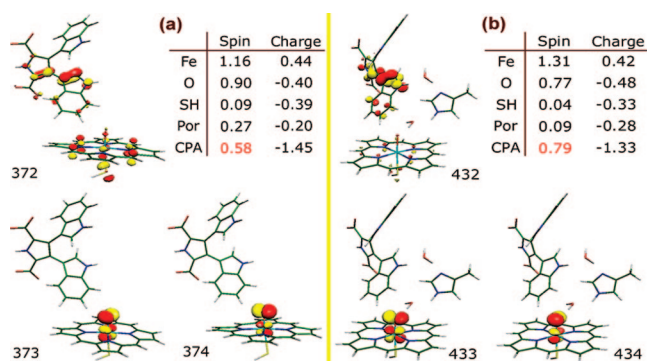


Figure 2. The singly occupied natural orbitals, Mulliken charges, and spin densities for the CPA–Cpd I complex (a) without and (b) with wat₇₈₉.

These tests verified that the H-bonding network modulates the extent of electron transfer (ET) from CPA to Cpd I, by analogy to CcP.^{5a} Strong H-bonds with the distal carboxylate prevented ET, while creating a H-bond path between CPA and the iron-oxo via the wat₆₄₄–His₂₅₀–wat₇₈₉ triad (Figure 1b) enhanced the ET from CPA to generate a Cpd II species analogous to CcP.^{5,9}

The facility of ET from CPA²⁻ to Cpd I may activate CPA.⁴ To screen potential initiating steps toward the transformation to **2** in Scheme 1, we performed exploration of three possible reactions. The first two reactions we considered were an initial decarboxylation and an initial aryl–aryl coupling. According to the energy scan (Figure S23 in the SI), initial decarboxylation will have a high barrier. With B3LYP/MM, C–C coupling was found to be endothermic by 19.3/20.3 kcal/mol, with a barrier of 22.2/23.4 kcal/mol with B1/B2, respectively. Interestingly, near the TS of the C–C bond formation, the electron transfer from CPA was completed and formed Cpd II.

Next we considered hydrogen/proton abstraction from the N–H bond by the iron-oxo species. As can be seen from Figure 1, the oxo is much too far to abstract a hydrogen species directly. However, if wat₇₈₉ can fill the space, there will arise an intriguing mechanism. Note that His₂₅₀ in Figure 1b and the water molecules wat₇₈₉ and wat₆₄₄ form a proton relay system typical of peroxidases.¹⁰ Indeed, in accord with our findings on horseradish peroxidase (HRP),¹¹ there occurs here too a proton-coupled electron transfer (PCET) step, whereby the CPA completes the ET to the *a_{2u}* orbital of Cpd I, while the indolic N–H is deprotonated by wat₆₄₄ that transfers the proton via His₂₅₀ to wat₇₈₉ and finally to the iron-oxo species to form the iron-hydroxo Cpd II isomer.^{11,12} The energy profile for this mechanism nascent from both the StaP/CPA¹⁻ and the StaP/CPA²⁻ systems is shown in Figure 3. For the StaP/CPA²⁻ system, the first proton transfer step from CPA to His₂₅₀ is endothermic and has a B2 barrier of 16.5 kcal/mol. The

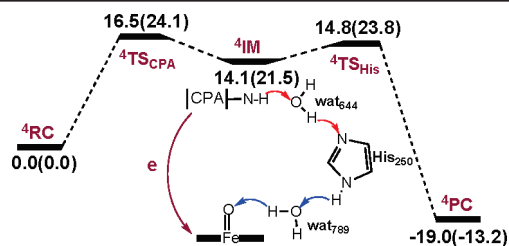


Figure 3. B3LYP(B2)/MM energy profiles (in kcal/mol) for the PCET process in the CPA²⁻/StaP and CPA¹⁻/StaP systems. Relative energies are given outside (inside) of parentheses for the CPA²⁻/StaP (CPA¹⁻/StaP) systems, respectively. Arrows indicate the direction of proton transfers.

second step is exothermic, and its barrier relative to MI is only 0.7 kcal/mol (which is reasonable considering the strong acid and the short NH–O distance), suggesting perhaps an effectively concerted process. Judging from the barriers of these three optional processes, PCET appears more favorable to start the sequence of events toward the transformation of CPA²⁻ to staurosporine, while C–C coupling provides an alternative path. Notably, starting from CPA¹⁻ (Figure 3), where no initial ET occurs, the mechanism is still PCET, but now it encounters significantly higher barriers, thus suggesting that CPA²⁻ is the actual active state of the substrate in the pocket.

In conclusion, the mechanistic hypothesis⁴ on the StaP-catalyzed conversion of CPA to **2** seems to be reasonable. In a favorable conformation of His₂₅₀, the active species of StaP is nearly a Cpd II species with a radical located on CPA, in analogy to the peroxidase CcP.¹⁰ Additionally, novel aspects were revealed: The ET is enabled simultaneously by His₂₅₀, the deprotonated carboxylate groups in CPA, and the H-bonding network that tunes the energetic of the process. The preferred protonation state of the substrate CPA was found to be dual-ionized and the reaction is initiated by overall PCET. The PCET chain is facilitated by His₂₅₀ that uses a peroxidase-like machinery.¹¹ Preliminary exploration shows that the initial PCET enables the full conversion of CPA to **2** by subsequent C–C coupling and proton transfers.

Acknowledgment. S.S. is supported by the ISF. H.H. is a JSPS Postdoctoral Fellow for Research Abroad.

Supporting Information Available: Thirty figures, eight tables, and Cartesian coordinates. This material is available free of charge via the Internet at <http://pubs.acs.org>.

References

- (1) (a) Ortiz de Montellano, P. R., Ed. *Cytochrome P450: Structure, Mechanism and Biochemistry*, 3rd ed.; Kluwer Academic/Plenum Publishers: New York, 2005. (b) Onaka, H.; Taniuchi, S.; Igarashi, Y.; Furumai, T. *Biosci. Biotechnol. Biochem.* **2003**, *67*, 127.
- (2) Howard-Jones, A. R.; Walsh, C. T. *J. Am. Chem. Soc.* **2006**, *128*, 12289.
- (3) Howard-Jones, A. R.; Walsh, C. T. *J. Am. Chem. Soc.* **2007**, *129*, 11016.
- (4) Makino, M.; Sugimoto, H.; Shiro, Y.; Asamizu, S.; Onaka, H.; Nagano, S. *Proc. Natl. Acad. Sci. U.S.A.* **2007**, *104*, 11591.
- (5) (a) Barrows, T. P.; Poulos, T. L. *Biochemistry* **2005**, *44*, 14062. (b) Sivaraja, M.; Goodin, D. B.; Smith, M.; Hoffman, B. M. *Science* **1989**, *245*, 738.
- (6) (a) Schöneboom, J. C.; Lin, H.; Reuter, N.; Thiel, W.; Cohen, S.; Ogliaio, F.; Shaik, S. *J. Am. Chem. Soc.* **2002**, *124*, 8142. (b) Schöneboom, J. C.; Cohen, S.; Lin, H.; Shaik, S.; Thiel, W. *J. Am. Chem. Soc.* **2004**, *126*, 4017. (c) Zheng, J. J.; Altun, A.; Thiel, W. *J. Comput. Chem.* **2007**, *28*, 2147.
- (7) (a) Schlichting, I.; Berendzen, J.; Chu, K.; Stock, A. M.; Maves, S. A.; Benson, D. A.; Sweet, R. M.; Ringe, D.; Petsko, G. A.; Sligar, S. G. *Science* **2000**, *287*, 1615. (b) Altun, A.; Shaik, S.; Thiel, W. *J. Comput. Chem.* **2006**, *27*, 1324.
- (8) Shaik, S.; Kumar, D.; de Visser, S. P.; Altun, A.; Thiel, W. *Chem. Rev.* **2005**, *105*, 2279.
- (9) For CcP Cpd I: Harvey, J. N.; Bathelt, C. M.; Mulholland, A. J. *J. Comput. Chem.* **2006**, *27*, 1352.
- (10) Poulos, T. L. *Nat. Prod. Rep.* **2007**, *24*, 504.
- (11) Derat, E.; Shaik, S. *J. Am. Chem. Soc.* **2006**, *128*, 13940.
- (12) Green, M. T.; Dawson, J. H.; Gray, H. B. *Science* **2004**, *304*, 1653.

JA711426Y